

From remote sensing of land cover and vegetation to data / model integration

Prof. Heiko Balzter
email: hb91@le.ac.uk

Global Climate Observing System (GCOS) Essential Climate Variables (ECV)

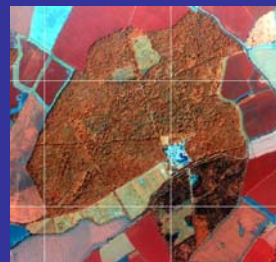
- Land related:
 - snow cover
 - glacier and ice cap extent
 - extent of permafrost and seasonally-frozen ground
 - land surface albedo
 - land cover (including vegetation type)
 - fraction of absorbed photosynthetically active radiation (fAPAR)
 - leaf area index (LAI)
 - biomass
 - fire disturbance
- [...]

Remote sensing approaches to mapping land cover and land use change

- Land cover classification
- Land use mapping
- Land surface properties:
 - Biomass
 - Vegetation height
 - Disturbances
 - Photosynthetic activity
 - Land surface temperature
 - Evapotranspiration

Overview of remote sensing satellites

- Optical/near-infrared



- Synthetic Aperture Radar



Earth Observation Satellites

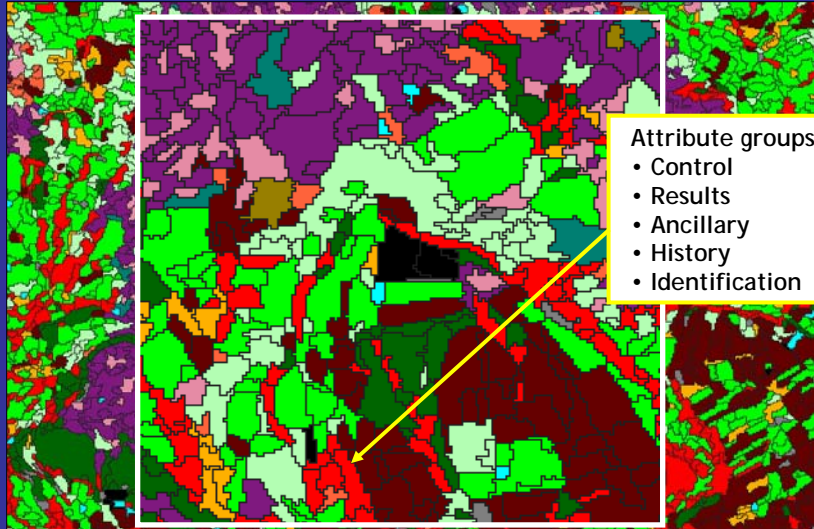
➤ Disaster Monitoring Constellation	➤ SAC-A	➤ TIROS-1
➤ IKONOS	➤ SAC-B	➤ TIROS-2
➤ QuickBird	➤ SAC-C	➤ TIROS-3
➤ SPOT	➤ SAOCOM	➤ TIROS-4
➤ EROS	➤ SPOT	➤ TIROS-5
➤ RapidEye	➤ ERS-1	➤ TIROS-6
➤ FORMOSAT-2	➤ ERS-2	➤ TIROS-7
➤ WorldView-1	➤ ENVISAT	➤ TIROS-8
➤ Aqua (EOS PM-1)	➤ IRS P6 (Resourcesat 1) 17 October 2003	➤ TIROS-9
➤ Aura	➤ IRS P5 (Cartosat 1) 5 May 2005	➤ TIROS-10
➤ GRACE	➤ IRS P4 (Oceansat 1) 27 May 1999	➤ Meteor 1 series
➤ Jason 1	➤ IRS P3 21 March 1996	➤ Meteor 2 series
➤ Orbview-2	➤ IRS P2 15 October 1994	➤ Meteor 3 series
➤ Terra (EOS AM-1)	➤ IRS P1 (also ID) (Crashed, due to launch failure of Polar Satellite Launch Vehicle, 20 September 1993)	➤ FY-1 series
➤ GOES 9	➤ IRS 1D 29 September 1997	➤ FY-2 series
➤ GOES 10	➤ IRS 1C 28 December 1995	➤ ALOS
➤ GOES 12	➤ IRS 1B 29 August 1991	➤ JERS-1
➤ NOAA-15	➤ IRS 1A 17 March 1988	
➤ NOAA-16	➤ GOSAT	
➤ NOAA-17	➤ TIMED (Thermosphere Ionosphere Mesosphere Energetics and Dynamics)	
➤ NOAA-18	➤ TOPEX/Poseidon	
➤ GMS-1 / Himawari-1	➤ Upper Atmosphere Research Satellite	
➤ GMS-2 / Himawari-2	➤ NOAA-4	
➤ GMS-3 / Himawari-3	➤ Vanguard 2	
➤ GMS-4 / Himawari-4	➤ BelKA	
➤ GMS-5 / Himawari-5	➤ Munin	
➤ Landsat 1	➤ MetOp	
➤ Landsat 2	➤ Meteosat 5	
➤ Landsat 3	➤ Meteosat 6	
➤ Landsat 4	➤ Meteosat 7	
➤ Landsat 5	➤ Meteosat 8	
➤ Landsat 6	➤ Meteosat 9	
➤ Landsat 7	➤ RADARSAT-1	
➤ CBERS-1	➤ RADARSAT-2	
➤ CBERS-2		
➤ CBERS-2B		

Based on Wikipedia (expanded)

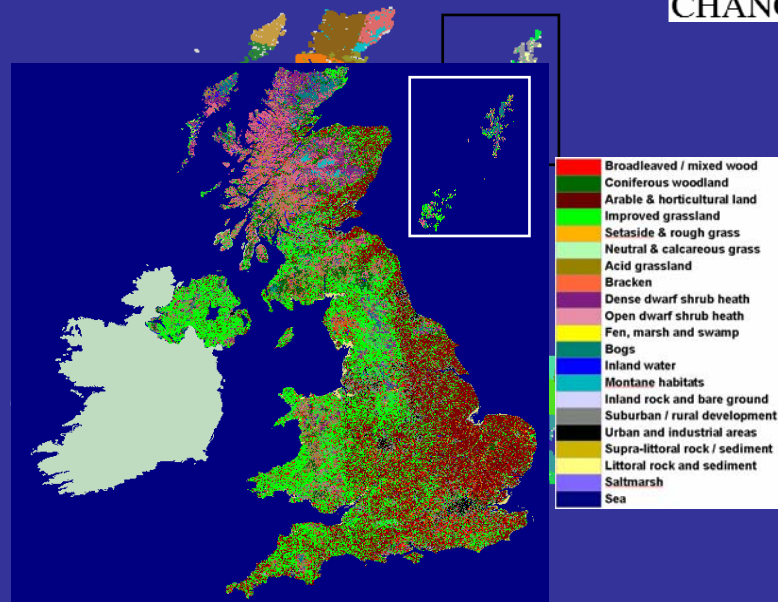
Land cover classification

- Traditional land cover maps are based on classified spectral images.
- Mostly optical / near-infrared sensors
- Characteristic spectral signatures for each land cover class
- Spectral class separability
- Pixel vs. parcel-based approaches

Classifying land parcels



Slide by Dr Geoff Smith



Slide by Dr Geoff Smith

Semantic uncertainties in quantifying land cover change

- To assess land cover change, one needs multitemporal maps of land cover.
- Often, these maps were made by different teams.
- Most have used different classification methods and labelling systems.
- This introduces semantic uncertainty.
- When comparing LCM 2000 to LCM 1990, about 80% of differences are due to semantic and methodological uncertainty.

What is a "forest"?

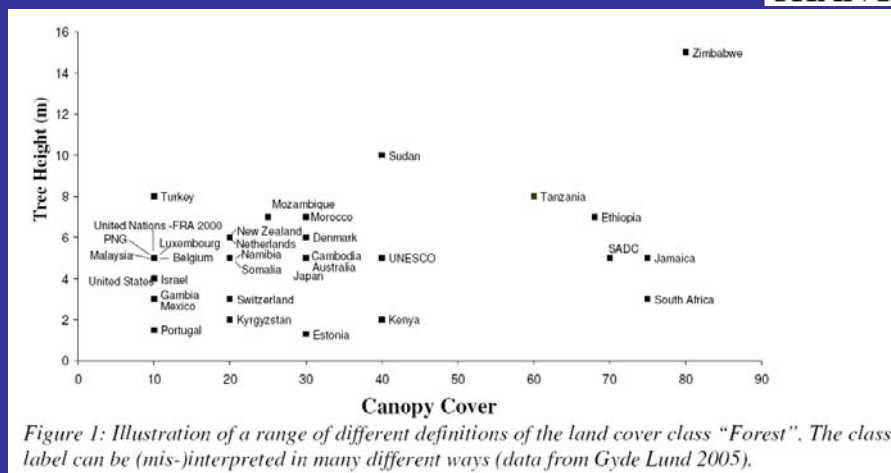


Figure 1: Illustration of a range of different definitions of the land cover class "Forest". The class label can be (mis-)interpreted in many different ways (data from Gyde Lund 2005).

From Wadsworth et al. (in press), Journal of Land Use Science
Data from:

GYDE LUND, H., 2005, Definitions of Forest, Deforestation, Afforestation, and Reforestation. Forest Information Services, Gainesville, VA, <http://home.comcast.net/~gyde/DEFpaper.htm>, date accessed: 27/9/2007.

Quantified conceptual overlaps (QCO)

- Two land cover classes “overlap” thematically.

$$O(p_A, p_B) = \frac{\int \min(f_{pA}(x), f_{pB}(x)) dx}{\int f_{pB}(x) dx}$$

$$O(p_A, p_B) = \frac{\sum \min(p_A, p_B)}{\sum (p_B)}$$

Domains used in QCO analysis

- photosynthetic activity/biomass accumulation
- wetness
- human disturbance,
- seasonality/phenology
- vegetation height

Table 2: Fragment of the table showing some classes in the “human disturbance” domain.

Human disturbance	Most Least									
Urban (s 3)	1	1	0	0	0	0	0	0	0	0
Urban (g27)	1	1	0	0	0	0	0	0	0	0
Urban and Built-Up (i13)	1	1	0	0	0	0	0	0	0	0
Croplands (s 4)	1	1	1	1	0	0	0	0	0	0
Cropland (g20)	1	1	1	1	0	0	0	0	0	0
Croplands (i12)	1	1	1	1	0	0	0	0	0	0
Humid Grassland (s 12)	0	0	1	1	1	0	0	0	0	0
Humid Grassland (g10)	0	0	1	1	1	0	0	0	0	0
Cropland Grassland Complex (g23)	0	0	1	1	1	0	0	0	0	0
Cropland/Natural Vegetation Mosaic (i14)	0	0	1	1	1	0	0	0	0	0
....
Sedge Tundra (g17)	0	0	0	0	0	0	0	0	1	1
Salt Pans (g29)	0	0	0	0	0	0	0	0	1	1
Barren Ground (s 2)	0	0	0	0	0	0	0	0	0	1
Bare soil Rock (g24)	0	0	0	0	0	0	0	0	0	1
Permanent Snow Ice (g25)	0	0	0	0	0	0	0	0	0	1
Snow and Ice (i15)	0	0	0	0	0	0	0	0	0	1
Barren or Sparsely Vegetated (i16)	0	0	0	0	0	0	0	0	0	1

Results

- Consistency between four land cover maps

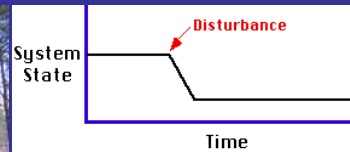
Table 3: Consistency between the SUC04 land cover map and three other maps (SUC03, GLC and IGBP) for selected test sites.

Site	Dominant cover(s) in SUC 04	SUC 03	GLC	IGBP
134023	Cropland/forest complex (49%)	95.4%	40.1%	41.3%
	Cropland (15%)			
143022	Cropland/forest complex (39%)	93.4%	50.1%	39.6%
	Deciduous broadleaved forest (25%) Croplands (21%)			
136021	Evergreen needle-leaf forest (44%)	71.0%	68.7%	73.7%
	Cropland/forest complex (35%)			
144020	Deciduous broadleaved (87%)	99.1%	98.4%	98.3%
137019	Evergreen needle-leaf forest (84%)	99.8%	99.6%	99.8%
143019	Evergreen needle-leaf forest (83%)	94.1%	99.2%	96.7%
129019	Deciduous needle-leaf forest (49%)	83.5%	60.3%	58.0%
	Tundra lichen-moss (25%)			
143017	Evergreen needle-leaf forest (60%)	95.9%	97.1%	90.9%
	Deciduous needle-leaf forest (36%)			

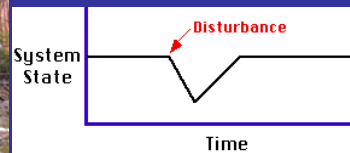
Disturbance monitoring



Photo by Daniel Smith

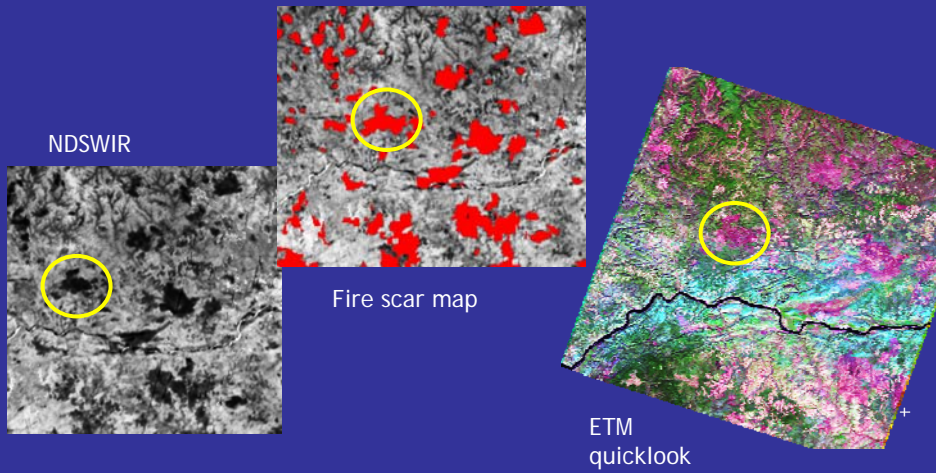


Unstable equilibrium

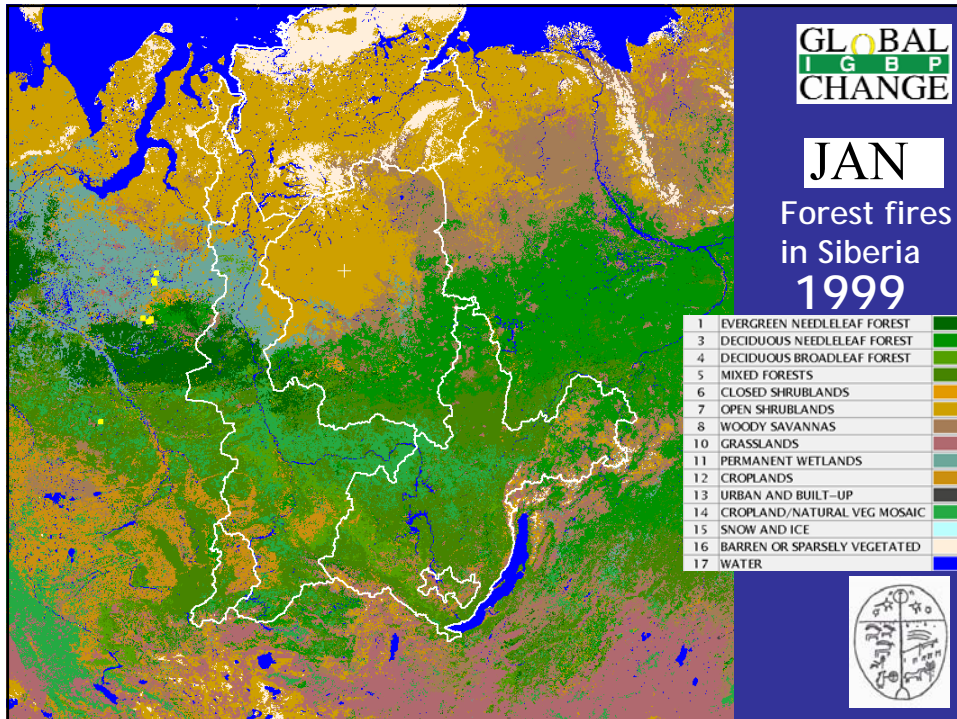


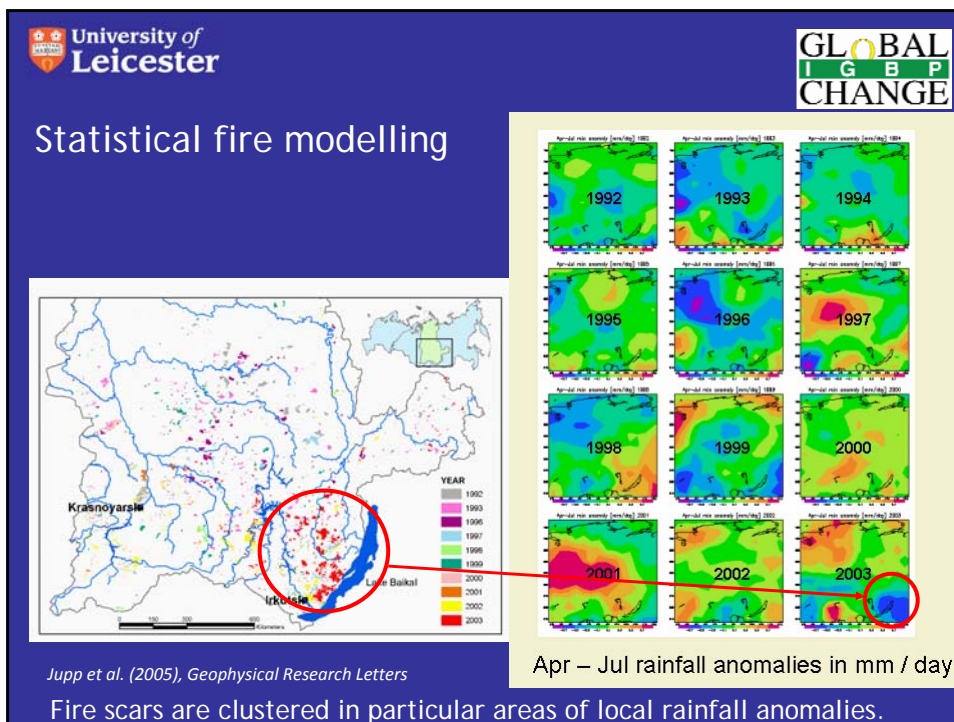
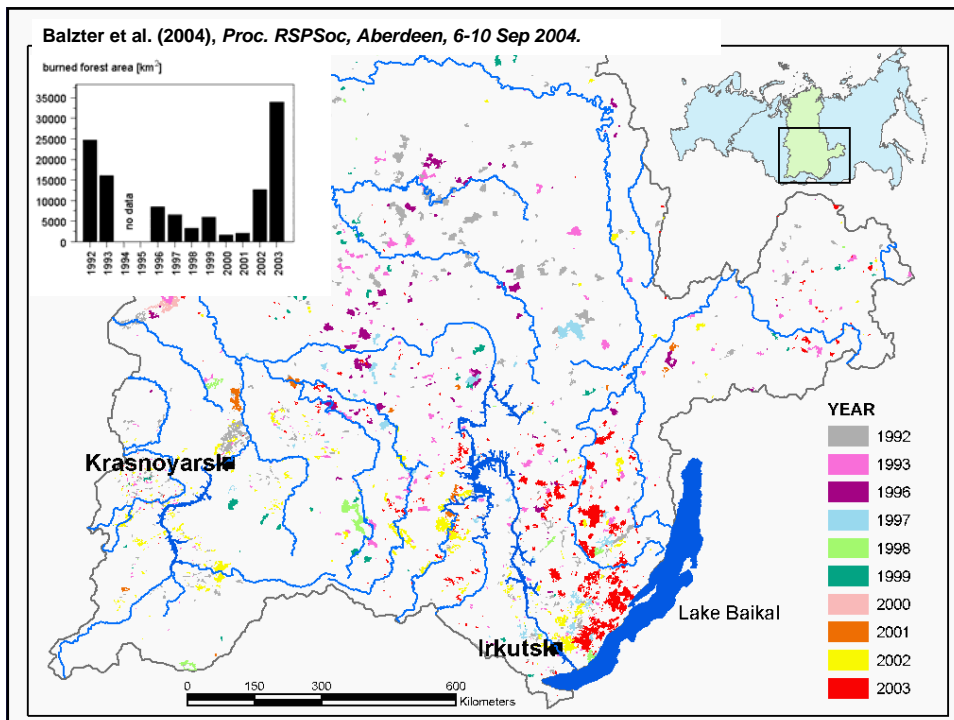
Stable equilibrium

Burned area mapping



Gerard et al. (2003), *IEEE Transactions on Geoscience and Remote Sensing* 41, 2575-2585





Statistical fire modelling

The number of fire scars within each grid box follows a negative binomial distribution.

$$P_n = \begin{cases} \frac{\Gamma(n + 1/k)}{\Gamma(n + 1)\Gamma(1/k)} \frac{(k\lambda_{ij})^n}{(1 + k\lambda_{ij})^{n+1/k}}, & k \neq 0 \\ \frac{\lambda_{ij}^n e^{-\lambda_{ij}}}{n!}, & k = 0 \end{cases}$$

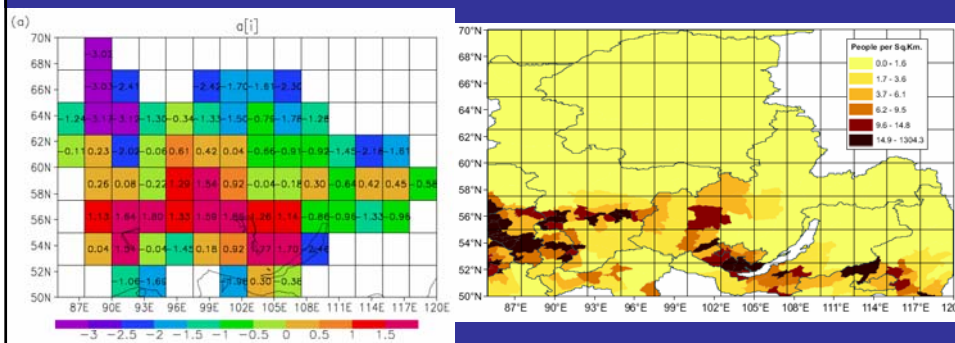
The rate λ is modelled as a function of grid box i , rainfall anomaly r_{ij} and year j .

$$\log(\lambda_{ij}) = a_i + b \cdot r_{ij} + c_j$$

All three factors were significant.

Jupp et al. (2005), Geophysical Research Letters

Causes of spatial heterogeneity

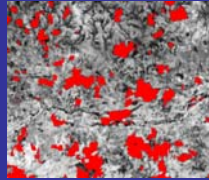


The grid box factor a_i correlates with population density (provided by Mike Bradshaw, Leicester).

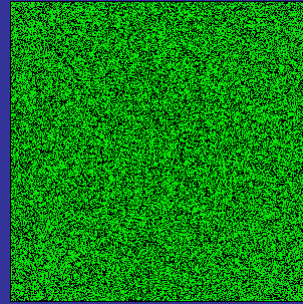
Humans are thought to be the greatest factor causing forest fires in the region.

Jupp et al. (2005), Geophysical Research Letters

Fire modelling with cellular automata



(satellite image)



- state space = {empty / tree / active fire}
- rules:
 - ignition probability = 0.00005
 - spread probability = 0.8
 - recolonisation probability = 0.1
 - 12 time steps in each fire season
 - extinguish all fires at end of fire season

Observations of vegetation phenology

Harmonic Analysis principles

- Time series is the sum of cosine waves of different frequencies.
- Each component wave is described by its amplitude and phase.
- Fast Fourier Transform produces series of complex numbers for each component:

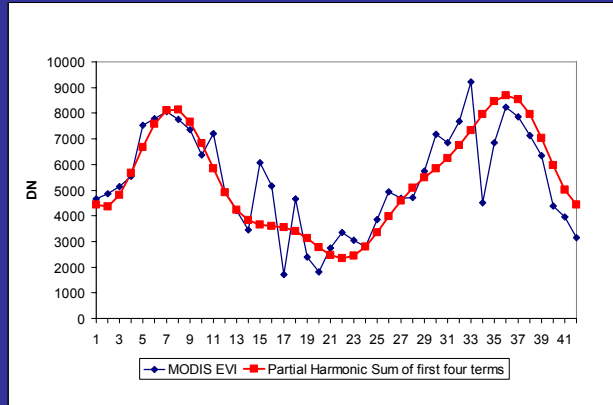
$$amplitude = \sqrt{img^2 + real^2}$$

$$phase = \arctan\left(\frac{img}{real}\right)$$

$$f(x) = real_j \cos\left(\frac{2\pi jx}{t}\right) + img_j \sin\left(\frac{2\pi jx}{t}\right)$$

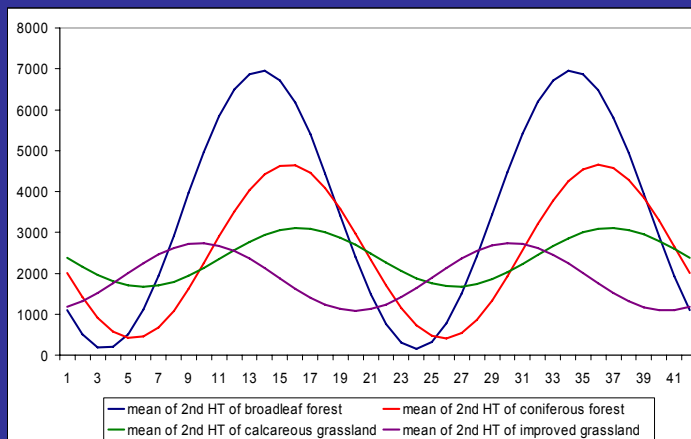
After M. Monreal

Harmonic Analysis applied



2 years of MODIS EVI data (8 day composites, 250 m pixel)
Author of slide: M. Monreal

Harmonic terms 1 to 4



Author of slide: M. Monreal

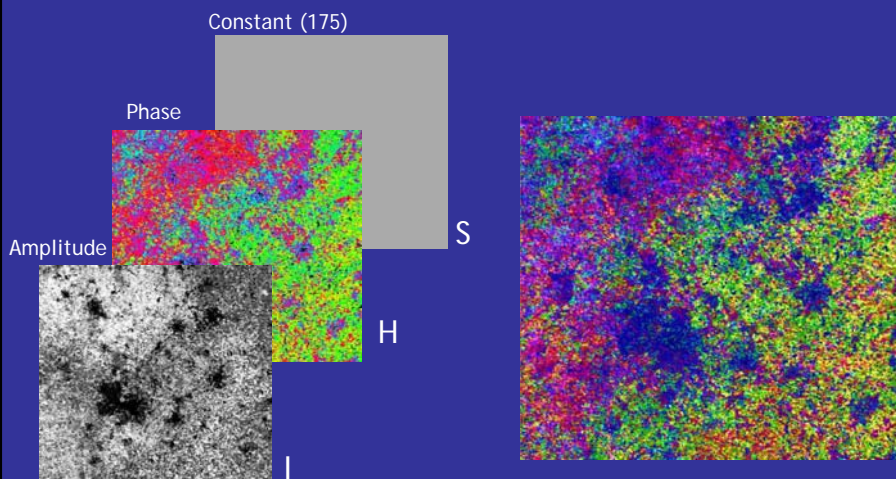
Visualising amplitude and phase

- Colour can be represented as RGB or IHS
- Amplitude on linear, phase on circular scale
- IHS representation of harmonic cycles (Hall-Beyer, 2003):

Intensity = amplitude (range of green-up)
Hue = phase (timing of max greenness)
Saturation = constant value (user defined)

Author of slide: M. Monreal

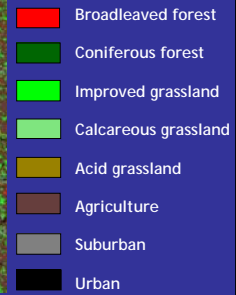
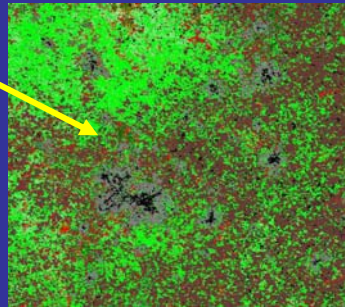
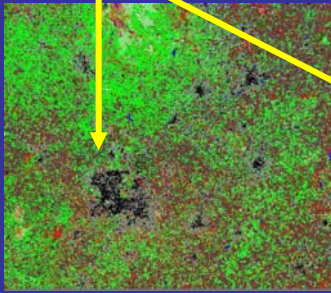
Amplitude and phase fusion image



Author of slide: M. Monreal

Comparison with land cover

Birmingham



UK Land Cover Map 2000 / Phenological map

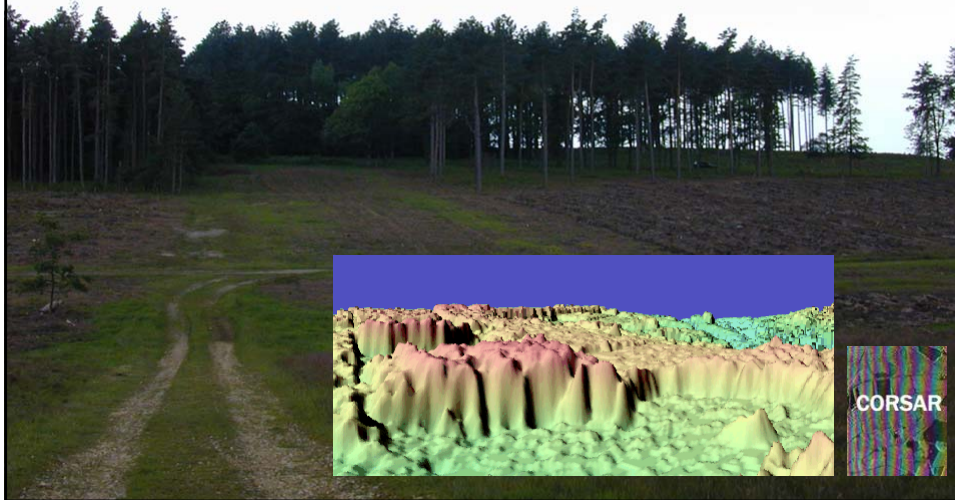
→ Land cover types have characteristic phenological traits.


Author of slide: M. Monreal

New methods for biomass mapping




Thetford Forest from SAR interferometry (X-band VV pol, single-pass E-SAR data)

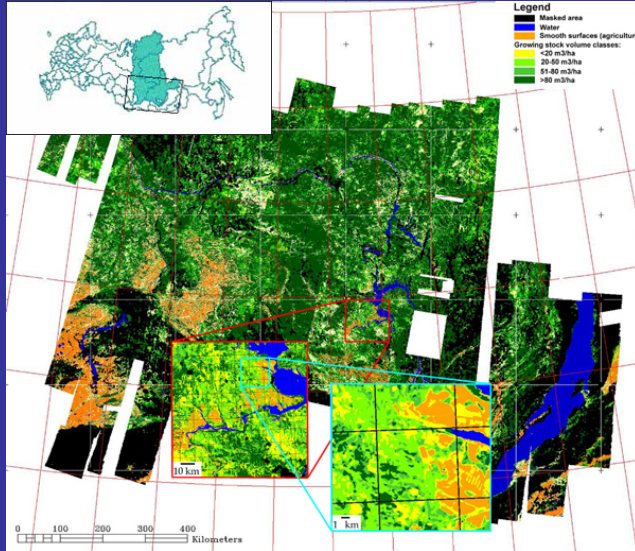




**University of
Leicester**



Siberia forest cover map




Legend

- Masked area
- Water
- Smooth surfaces (agriculture)
- Growing stock volume classes:
 - <20 m³/ha
 - 20-60 m³/ha
 - 61-80 m³/ha
 - >80 m³/ha

Produced using
600 ERS-1/2 and
JERS-1 SAR
images

Forest biomass
classes

Area of 1m km²



Balzter et al. (2002), *Canadian Journal of Remote Sensing* 28, 719-737.

Issues

- Traditional land cover mapping can now be complemented by new remote sensing techniques.
- GMES could provide consistent and compatible land cover change data for the first time.
- What information is required by land use modellers (time and space resolution, accuracy etc.)?